

REVIEW OF CHALLENGES AND OPPORTUNITIES IN LASER BEAM POWDER BED FUSION OF PLATINUM ALLOYS

Dr. Chloe R. Cunningham, Alloy Design - Programme Manager

Charles Knottenbelt, Laurent Beirnaert, Karol Murawski, John W.G. Clark, Fauzan Adziman

> Alloyed Oxford, UK

INTRODUCTION

Despite being proven able to produce high-quality jewellery pieces and the numerous potential advantages of additive manufacturing (AM) such as efficient material usage, and design freedom, Metal Laser Powder Bed Fusion (LB-PBF/M) (ISO/ASTM 52900, 2021) remains a niche technology. Bridging the gap between existing reviews and the current landscape of the technology, this paper will explore the underlying causes for this and take a deep dive into an underexplored limitation of additively manufactured platinum so far: the ability to efficiently engineer the AM production of unknown jewellery designs and, inherent to this, the ability to predict and correct build defects a priori.

Avoidance of thermal defects in LB-PBF/M and strategies for enhancing part quality through build file preparation, support structure attachment and post-processing are reviewed. A commentary on alloy behaviour and insight into the enhanced process-microstructure-property relationship observed in additively manufactured Platinum Ruthenium 950 alloy (PtRu950) are provided. As additive manufacturing continues to transform industries, the insights from this paper intend to contribute to advancing platinum LB-PBF/M's capabilities and adoption for jewellery applications.

1. The economic case for LB-PBF/M of platinum jewellery A major driver of the economic case of additive manufacturing is the ability to manufacture complex geometries efficiently, with minimum losses of material during the process. For example, within the Oil and Gas, Aerospace and Space industries, despite the

hurdles in satisfying safety and certification requirements change manufacturing processes, additive manufacturing is becoming widely adopted as a necessary technology required to remain competitive from a production cost and sustainability perspective.

Given the jewellery industry demands highly complex features and platinum alloys are considered difficult to process by traditional processing routes, incurring high material losses and costs of waste throughout the process, at first glance, it may seem unusual why AM has not seen more widespread adoption. By producing near-net shape components, material removal and refining are reduced compared to CNC machining and investment casting via machining chips and sprues, respectively, a concept known in the Aerospace industry as the Buy-to-Fly ratio. For platinum jewellery production, this can translate to reduced refining losses and potentially lower overall precious metal inventory. Zito previously covered the economics of the process, showing that the LB-PBF/M has the potential to rival investment casting fabrication on a like-for-like basis (Zito et al., 2018).

Beyond this, operational advantages can also be achieved, conventional production routes can often involve complex, multi-step activities, requiring large batches and heavy machinery e.g., ingot pouring, rolling, and stamping machines. LB-PBF/M provides greater control and repeatability compared to investment casting, a process that is known to be unreliable (Atkin, 1996; Frye & Fischer-Buehner, 2012). For product types like wedding bands and watch components, which depend on preformed input materials of certain dimensions such as tubes, LB-PBF/M can improve manufacturing scheduling flexibility and supply chain complexity by the direct provision of complex near-net components. This opens the opportunity for digital inventories, where batches can be produced according to customer demand.

Whilst, indeed, AM generally can produce highly complex parts, depending on the suitability of the part for AM manufacture, the engineering and design costs can vary widely. Producing parts with features and requirements unideal for AM can incur a cost penalty. To resolve these difficult-to-manufacture features, feedback on design suitability is often required to limit engineering effort and enhance manufacturability, and for this reason, education in design-for-AM (DfAM) remains a major opportunity in growing the use of AM in the jewellery industry.

In some cases, the DfAM rules are straightforward, and designers can plan around the new AM manufacturing rules e.g. it is well-

known that overhanging geometry must be attached to the build plate by sacrificial support structures to prevent the wiper from dislocating the geometry and to provide pathways of thermal conduction that enable the development of a stable melt pool and subsequent part geometry. Additionally, foresight of support structure removal and the following finishing processes is key to establishing whether the sacrificial support volume and locations are sufficient and optimal or whether an engineering or design change is recommended. Designers working with LB-PBF/M service bureaus can take into LB-PBF/M dimensional limitations and design around these to avoid issues regarding feature definition and finishing. As reported by Ferraro (2023) in a recent Metal AM article there are increasing numbers of jewellery designers who are designing for the AM technology, incentivized by the ability to curate new design aesthetics and topologies, as well as leverage the excellent compatibility of platinum and the LB-PBF/M. This trend is expected to continue in the coming years.

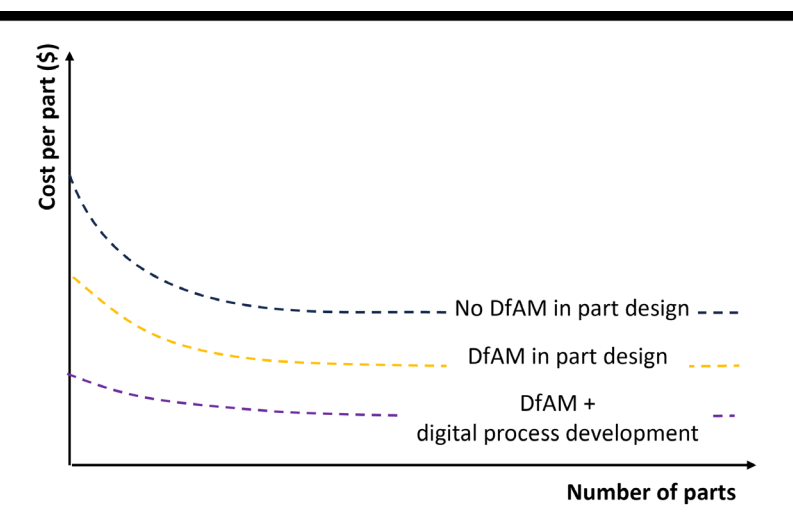


Figure 1: Relationship between the readiness of the part design to be manufactured by AM and cost compared to conventional processing

However, often defects that occur during the LB-PBF/M process can be difficult to predict via expertise alone and physical production trials are needed to establish true manufacturability. During a trial to establish a production pathway, the engineering of the AM production is optimised. If during the process the engineering toolbox fails to resolve production challenges, part design modifications and costly iterations of this process may be needed. Given that creative design intent is of utmost importance within the luxury, jewellery and consumer industry, design changes at this

point may be unacceptable. Moreover, for every trial print, high material and non-recurring engineering costs are incurred, which must eventually be offset by the retail sales price. Consequently, this upfront non-recurring engineering requirement can limit the process as economically competitive only for high-end, higher volume batches, where the initial development cost can be recuperated. This outlines a requirement to move away from physical experimentation to digital process development to democratize the technology for smaller, more mainstream production batches.

Whilst there are several factors alongside this upfront engineering effort that are hindering the wide-scale adoption of LB-PBF/M AM these topics are well covered by previous works. For example, research can be found on challenges of powder production(Jörg Fischer-Bühner, 2023; Laag & Heinrich, 2018) and resolution and additional finishing requirements (Fletcher, 2018; Zito et al., 2022). Moreover, for the fundamentals of processing platinum with LB-PBF/M there have been several investigations covering many aspects of the process development for platinum (Held & Klotz, 2022; Zito et al., 2015, 2018, 2022). This paper will therefore focus on the topic of thermal management, which, due to its negative impact on part quality and product development cycles, can be viewed as a significant factor hindering wide-scale adoption of LB-PBF/M for platinum jewellery production.

2. Printing challenges and thermal accumulation related defects in LB-PBF/M of platinum

The challenge of thermal accumulation defects in platinum LB-PB-F/M has been briefly touched upon in previous literature. Laag & Heinrich, 2018 discussed how bulky or fillagree components have different limits in thermal dissipation that can cause pores and deformations due to residual stresses. Klotz & König, 2022 reported the presence of an unexpected defect on the down-skin region of a seemingly uncomplex build of a solitaire ring. This section of the paper will explore further the rationale for thermal-induced defects and present potential solutions for their resolution. Thermal accumulation-induced defects can occur when the combination of build file configuration (part orientation, build layout, laser parameters) and part geometry combine unfavorably to prevent stable melting and dissipation of the heat away from the melt pool. This can occur both at a global level (part scale with thermal accumulation layer by layer) and at a local level (thermal accumulation within a toolpath or layer).

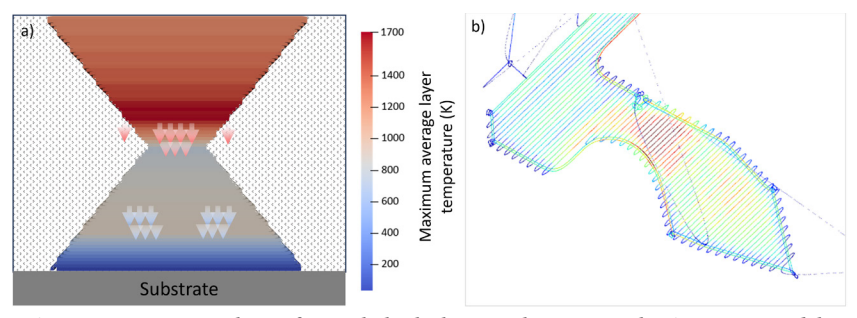


Figure 2: Examples of a) global thermal accumulation caused by varying scan area layer by layer and b) example of a localized thermal accumulation caused by short scan path lengths (within layer scan paths shown, red is hotter)

Both global and localized heating is influenced by the part geometry and its orientation in which the part is heated and supported as these factors define the thermal boundary conditions during the print process. Areas which do not have a sufficient thermal conductance pathway can be susceptible to overheating. One such example of this is shown in Fig. 3a) where down-skin regions built at an overhanging angle are shown. These do not have underlying solid bulk material with which to conduct heat away and rather conduct the heat mostly through the underlying loose powder, with significantly lower thermal conductivity. This can lead to greater heat build-up in these regions and consequently, there can be a tendency for greater surface roughness caused by the attachment of semi-sintered particles. In contrast, Fig 3b shows the thermal conditions in up-skin regions where conductance through the bulk material is available through prior underlying layers of material.

Although overhangs are one of the better-known examples of features known to cause overheating, the phenomenon is not uniquely linked to them and may occur even if overhang design guidelines are explicitly followed (Ranjan et al., 2020). This indicates that not only the local overhang angle but also the thermal response should be considered for detecting and preventing overheating. It can be helpful to consider the concept of thermal choking: how much opportunity does a local area of the AM component have to evacuate its heat? Features which involve a transition in geometry as the build progresses from a relatively small scan to a large area have a propensity to thermal choking. Therefore, the features which may also be problematic for thermal choking include the transition zones between often fine support structures and bulk component printing and filigree/lattice details which transition back to bulk material within the component as builds progress.

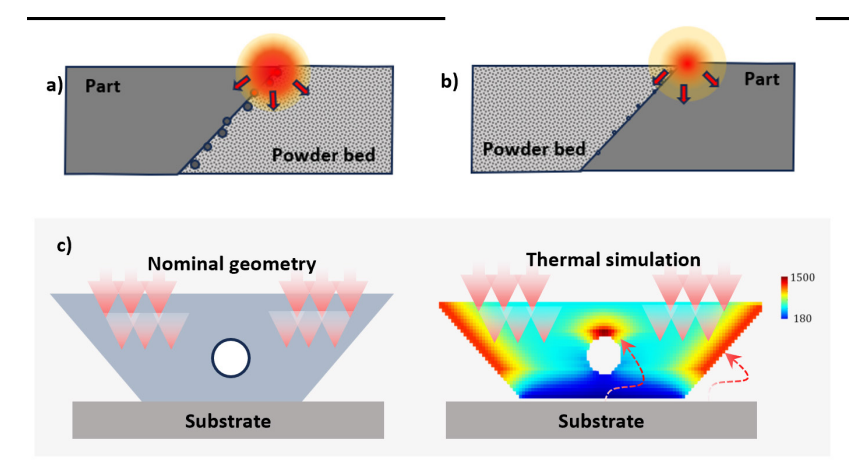


Figure 3: Schematic of thermal conductance pathways for a) downskin region b) upskin region c) Predicted heat accumulation for a test geometry component showing around the unsupported hole feature and down-skin zones.

Beyond the worsening of the surface roughness, thermal-related defects are important to avoid as they can also cause significant deviation from the nominal geometry and other issues such as porosity during the AM process, which means the desired 3D geometry cannot be realised to specifications. This can occur when thermal accumulation results in the expansion of the melt pool to a degree that additional powder is absorbed into the melt pool during the printing process resulting in a build-up of material. This can lead to errors in the spreading of the powder and geometric deviation. A typical example of this is shown in Fig 4a where the transition zone between supports and the ring shank of the part resulted in unstable material printing for which the build had to be stopped. This is of course an undesirable outcome, lowering the yield of the LB-PB-F/M process and increasing production costs and times.

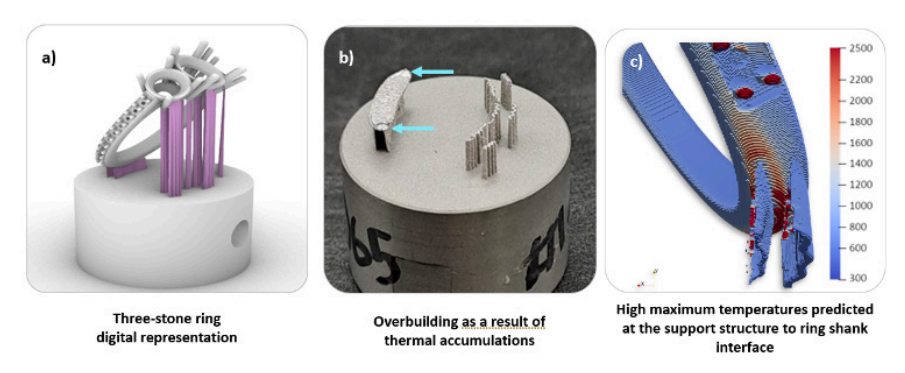


Figure 4: example of a failed build due to severe thermal accumulation a) digital representation b) experimental result c) retrospective thermal simulation highlighting severe maximum temperatures in the failure zone.

Aside from build failures, thermally induced defects may result in surface deformations from the planned nominal geometry which can require additional reworking efforts after printing. An example of this effect is shown in Figure 5, where a shrinkage line defect has occurred with a deviation of approximately 200µm from the best-fit nominal geometry. The possibility of a surface defect or build failure can be predicted by thermal simulation tools as shown also in Fig. 5. The technical annex provides further information on the methodology used for simulating the thermal profile and generating the corresponding hotspot index.

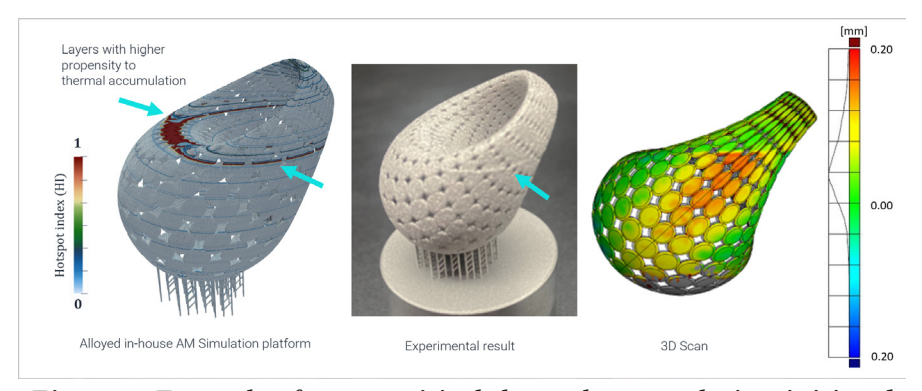


Figure 5: Example of a non-critical thermal accumulation-initiated line defect caused by significant local heating.

2.1 Approaches for avoiding thermal defects

2.1.1. Orientation optimisation

Optimizing the build orientation of the part ahead of printing is one of the key decisions within the part preparation workflow and influences various facets of the manufacturing process, including print duration, support structure requirements, thermal distribution throughout the build and, ultimately, the quality of the manufactured part. Additionally, it directly affects the efficiency of the printing process, impacting the time required for completion. The thermal profile during the build is intricately tied to part orientation, and consequently, orientation can be seen as one of the key methodologies for optimizing the thermal profile to avoid heat-related defects. The impact of the orientation on the types of thermal profiles for a typical ring geometry is shown in Figure 6.

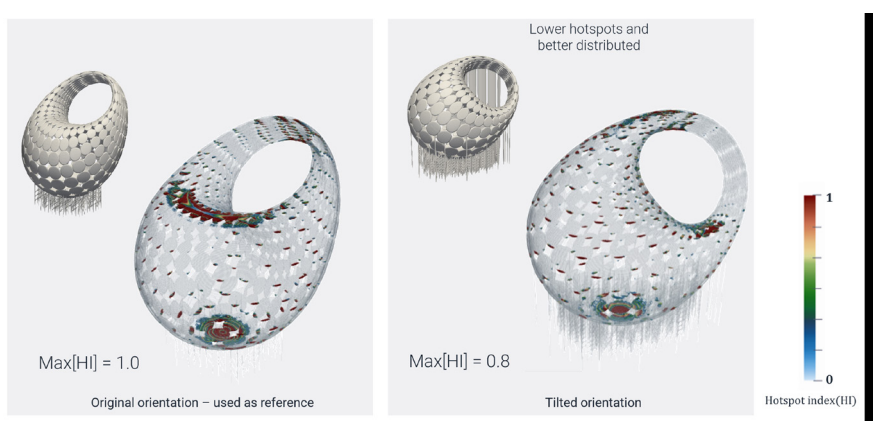


Figure 6: Example showing how the thermal hotspot profiles can vary with different build orientations.

2.1.2 Support structure optimisation

In 2015, Zito et. al. emphasized the critical role of support structures in laser powder bed fusion (LPBF), particularly in ensuring part stability during printing and facilitating effective thermal management. These support structures not only secure the part from disturbances caused by the printing wiper but also establish essential thermal pathways throughout the printing process. Consequently, the operator's expertise becomes paramount in optimizing print quality by strategically orienting the object on the printing platform to minimize reliance on support structures, thus reducing the areas affected by them. The operator must also consider the nuances of the thermal profile to make informed decisions regarding support structures. While adding extra support material can serve as a practical solution to enhance thermal conductivity. it also leads to increased post-processing efforts to remove excess material and extends printing durations. Therefore, striking a balance between effective thermal management and minimizing production waste becomes a crucial consideration in LPBF operations.

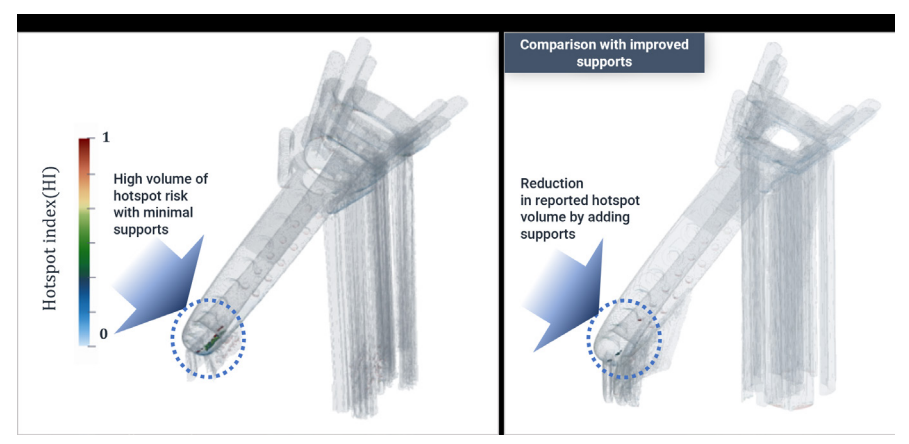


Figure 7: Demonstration of the decrease in volume of hotspot risk areas reported before and after support structure reinforcement.

2.1.3 Advanced laser tool pathing control and machine set-up Besides orientation and support structure optimisation, there is the opportunity to manage thermal accumulations through the control

opportunity to manage thermal accumulations through the control of the laser parameters such as power, hatch distance, scanning speed and layer thickness. Currently, widely used software can segment the part geometry into bulk, up-skin and down-skin, areas to specifically control the process parameters in these areas to balance speed and productivity with the density of the material produced. A downside of this current approach is that often processing parameters that are optimised for high density and not optimal for thermal management and there may be some trade-off with density in building parts that experience severe thermal accumulations. Other strategies for enhanced thermal management may also include the selection of substrate material for high conductivity, e.g. the use of copper. However, this approach is limited in effectiveness the further the build proceeds away from the substrate. LB-PBF/M engineers also have at their disposal the option to select from an array of scanning strategies. Future research activities in this area will include further segmentation of the part by process parameters for thermal management and resolution control.

3. Rationalising the mechanical properties of LB-PBF/AM PtRu950

For PtRu 950 alloy, excellent properties have been reported in comparison to casting processes. Comprehensive research of mechanical properties was covered by (Frye et al., 2023) detailing microstructure features and tensile properties in both as-built and hot isostatic pressing (HIP) post-processing condition. Several researchers have commented that high density is achievable within platinum LB-PBF, which is commonly attributed to the good

balance of reflectivity and thermal conductance which allows the development of a stable melt pool(Held & Klotz, 2022). The higher hardness, in combination with virtually zero sub-surface porosity, presents the opportunity of translating to more productive machining processes, with less rework such as deburring and laser welding. This section will take an in-depth view of the microstructural developments during the LB-PBF/M process.

3.1 Linking microstructural features to hardness

The microstructure of LB-PBF-produced material is typically more refined than the cast counterparts. The rationale for this lies in the extremely high cooling rates of 105 - 108 K/s that occur during the process, which are a result of the rapid movement of the laser within the scan field in combination with a fine spot size of between 30 µm -120 µm. (Zito et al., 2015) previously found grain size in LB-PBF/M platinum alloy of approximately 30 µm in the region of a third of that found in equivalent investment cast alloy. Grain refinement is known to increase the yield strength and hardness of alloys as the additional grain boundaries impede the travel of dislocations resulting in higher strength according to the Hall-Petch relation. Hardness testing of the as-built LB-PBF/M and cast material shows that there is an increase in hardness of approximately 25% within the LB-PBF/M PtRu material which aligns very closely with previous work (Frye et al., 2023).

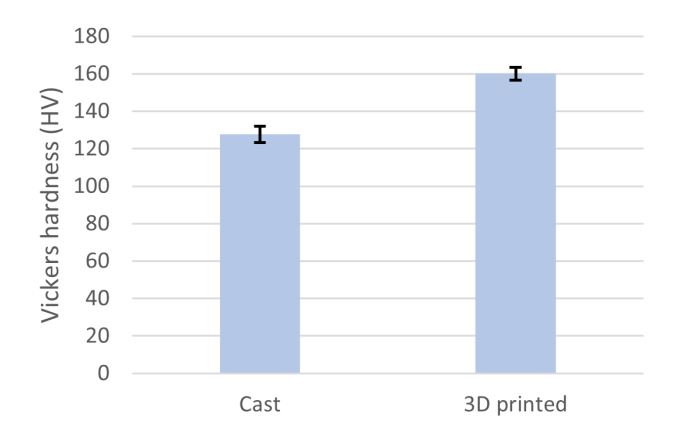


Figure 8: Hardness indentation measurements conducted at Alloyed for cast and LB-PBF/M PtRu950 material

To explore further the relation of microstructure to hardness property, electron-backscatter diffraction (EBSD) imaging was used to inspect the differences in grain distribution and orientation of growth between AM and cast Pt950 alloy. To investigate microstructure development with thermal profile, specimens were

designed to deliberately initiate varying degrees of thermal choking during printing to allow inspection of microstructures with different thermal histories. This was achieved by the specimens having different stem thicknesses which would cause a greater and lesser extent of conduction to the build plate during the LB-PBF/M process.

EBSD was selected as an analysis technique rather than etching to reveal grain boundaries, as EBSD can additionally inform us of the direction of the crystalline grain growth and enable rapid and precise calculation of grain size and orientation. This is of use as crystals demonstrate varied properties depending on their growth direction, and with the strong thermal gradient, crystal growth can be encouraged in one direction in additive processes leading to anisotropic, inhomogeneous mechanical properties.

Prior to analysis the samples were set in conductive resin and ground to a mirror finish, ending on 0.04 μ m colloidal silica. The analysis was performed on a Tescan MIRA 4 scanning electron microscope (SEM) equipped with an Oxford Instruments C-Nano camera, an accelerating voltage of 20kV, beam current of 10nA, and a scanning step size of 2.5 μ m. EBSD analysis for the two most extreme cases (1mm stem 30° overhang, 3mm stem 45° overhang), with the inverse pole figures highlighting crystal texture relative to the build axis, are shown in Figure 9.

It can be observed from the EBSD scans that there is a relatively weak texture in the build direction, with a stronger general texture shown in the <101> direction on the x-y plane, which may be a result rapid cooling of the grains growing in the direction of the laser scan path. The specimen with more extreme thermal choking was found to have a lower multiple of uniform density overall (more random texture and closer to a polycrystalline microstructure) but with a slightly higher tendency to <001> grain growth along the build direction.

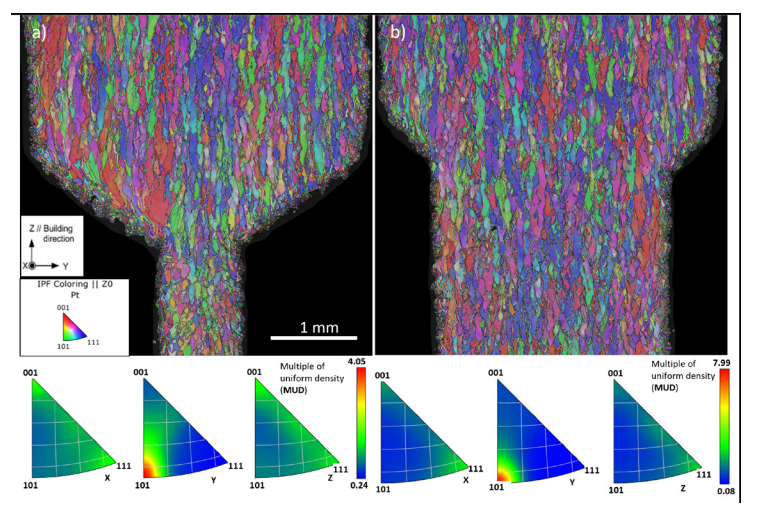


Figure 9: IPF EBSD images of thermal choking specimens showing microstructure variations along the build direction (z).

Mapping the Vickers microhardness across the thermal choking coupon zones as shown in Figure 10, showed for all specimens that the hardest areas were the bulk cube region and the least hard areas corresponding to the necking area between cube and stem. The coupons with the most severe thermal choking displayed the largest decrease in hardness up to 15% lower compared to the areas that did not experience any thermal accumulations.

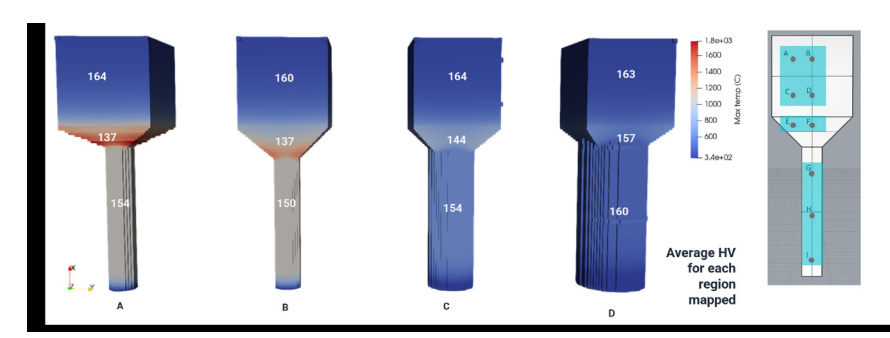


Figure 10: Hardness test results shown superimposed onto thermal simulation showing some correlation between lower hardness and thermal accumulation hotspots.

Within the choking zone of the 1mm stem, 30° overhang thermal choking specimen, it can be seen in Figure 10 that there is variation in the grain texture and size across the thermal choking zone with the left-hand side of the specimen showing larger grains, which are more oriented towards the <001> grain growth direction which is indicative of high levels of thermal accumulation and pro-

motion of grain growth along the build direction.

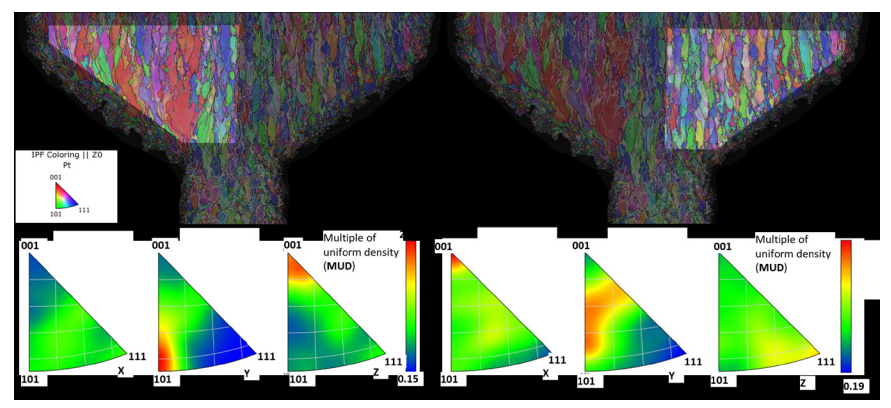


Figure 11: IPF EBSD images of sub-sets of the 1mm stem 30° overhang angle thermal choking specimens showing textural variation across the thermal choking zone.

As the crystal texture within a face-centred cubic (FCC) material impacts the linear elastic properties of a material, these variations in texture therefore are subsequently relevant for mechanical properties of PtRu 950 LB-PBF/M samples including hardness. The Zener's coefficient for cubic crystals represents how significantly the material will display anisotropy in mechanical properties with the development of strong crystal texture, with one being equivalent to polycrystalline material. In FCC materials, most cubic metals have a positive value of Zener's Anisotropy factor so that the <001> grain growth direction is soft and <111> is hard. For platinum, the Zener Coefficient of 1.59 can lead to high elastic modulus variations between the <001> and polycrystalline uniform texture of ~40 GPa as shown in Table 1.

Table 1: Voigt-Reuss average value of in-plane Young's Modulus for polycrystalline and <001> grains and anisotropy factor reported for a selection of fcc metals.

Face-centred cubic	Young's Modulus (GPa)		Zener's Anisotropy
elements	001 texture	Uniform texture	factor
Al	63	70	1.22
Ni	129	221	2.67
Si	130	163	1.55
Pt	136	177	1.59

This is significant for material built by LB-PBF/M regions that have experienced thermal accumulations have the tendency to develop a textured growth of grains along the <001> direction is likely to

result in some differences in mechanical behaviour such as lower hardness and modulus, which can in turn affect end-use performance. Besides the textured <001> grain growth which is known to be less hard in platinum alloys and higher heat and slower cooling rates can promote the formation of larger grains which would also result in lower hardness contribution from Hall-Petch strengthening. Furthermore, in-process annealing can be considered a possibility because of the elevated temperatures in this zone, which can also result in recrystallisation and grain growth dynamics as well as the reduction of the strain contained within the material and the contribution from dislocation strengthening.

Further inspection of the microstructure shows asymmetric grain growth along one side of the thermal choking zone. Pyrometry data was collected during the LB-PBF/M process which records the emissivity signal and can be correlated with local temperature during the build. This is shown for the thermal choking specimens within the region where thermal choking was predicted to occur in Fig. 12. Reviewing the scan-path temperature pyrometry results, asymmetric heat build-up across the scan-path is displayed, with the average maximum temperature per voxel increases as the scan path progresses from the top right corner to the bottom left corner, with the samples with the finer stems and more extreme overhangs more greatly affected.

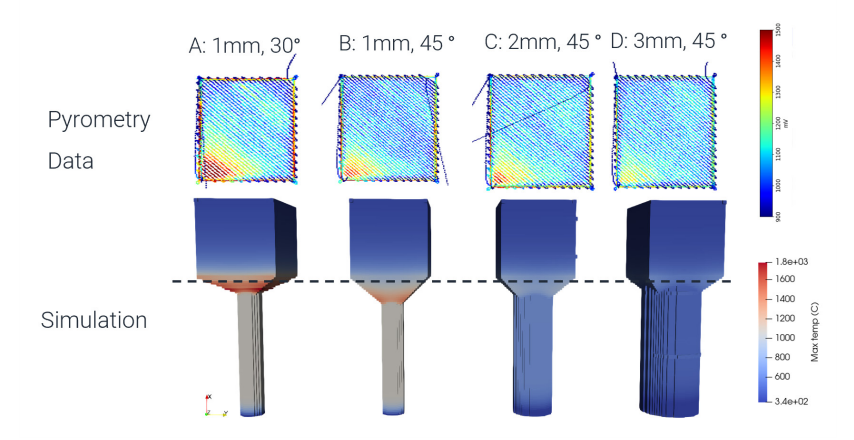


Figure 12: Pyrometry data showing the asymmetric thermal accumulation within a layer during LB-PBF/M of the thermal choking coupons.

This result is significant as it indicates that the local scan-path accumulation within the globally predicted choking region also appears to be impacting microstructural development and consequently hardness and other mechanical properties. In addition,

Kernel Average Misorientation (KAM) maps as shown in Fig 13 show a notable decrease in the KAM measurement within the outer skin of the thermal choking region. KAM is an indicator that may be extracted from EBSD analysis, which is representative of the strain and dislocation strengthening embodied within a sample, which indicates some in-process annealing is indeed apparent as a consequence of the combination of global and local heating phenomena.

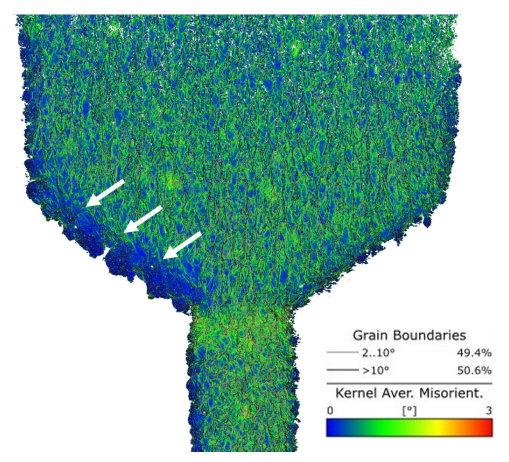


Figure 13: Kernel Average Misorientation map for the 1mm stem, 30° overhang angle thermal choking specimen showing a decrease within the localised thermal accumulation region.

These results are relevant to the industrialization of platinum by LB-PBF/M as consistent material properties are necessary for high volume, production scenarios. This work has highlighted that those mechanical properties and hardness properties should be mapped within a certainty window that is proportional to the thermal history of the component. A more in-depth understanding of the tolerance of mechanical properties will ensure parts can be produced as expected, to facilitate wide-scale industrial production.

4. Conclusions

This paper has highlighted the current challenges with regard to the wide-scale production of LB-PBF/M platinum components. The main findings may be summarised as follows:

- The thermal profile of LB-PBF/M is adaptable and dynamic throughout the LB-PBF/M process and influences the microstructural features and consequently can be expected to impact the mechanical behaviour and wear resistance of PtRu950 jewellery pieces.
- Thermal accumulations during LB-PBF/M are a potential

source of surface roughness, surface deformations and build failures, and present a challenge to overcome as part of the process development. The accumulations can be managed by the addition of support structures, consideration of part orientation and modification of scan strategies.

- AM and LB-PBF/M of platinum can currently require reworking or iterations of the design or re-engineering of the original build file as well as several iterations before the design can be considered production-ready, much of which depends on designers' and operators' engineering expertise and experience. A more advanced digital toolset is required to assist engineers in preparing correctly built files to balance not only surface roughness and cost but also to manage thermal accumulations.
- A paradigm shift from experimental AM product development to digital AM development cycles is expected to resolve complex heat-related defects a priori. Incumbent technologies will shift the economics of LB-PBF/M to improve the quality and scalability of platinum AM.

5. Technical Annex: Method for predicting hotspots during LB-PBF/M Process

The Alloyed Solver platform performs part-scale thermal modelling of the additive manufacturing process with the aim of predicting features that can cause thermal hotspots. To do this, the Solver platform offers a range of simulation fidelities that provide an optimal balance between computational efficiency and accuracy. Local overheating or heat build-up is a well-known problem in powder-based additive processes and can lead to poor properties, poor surface quality and build failures. The heating or cooling cycles experienced during the process cause thermal expansion and contraction, ultimately leading to the development of residual stresses that cause significant distortion in the final part. During manufacturing process, the temperature T in an AM part varies according to the following partial differential equation (PDE)

$$\rho(\mathbf{T})c_{\mathbf{p}}(\mathbf{T})\partial\mathbf{T}/\partial\mathbf{t} = \nabla \cdot (\mathbf{k}(\mathbf{T})\nabla\mathbf{T}) + \mathbf{Q}_{\mathbf{v}},$$

where t is time, Q_v is the heat source and $\rho(T)$, c_p (T), k(T), are the temperature dependent density, specific heat and conductivity, respectively. This PDE is solved numerically within the Alloyed Solver platform and the resulting temperatures are found. The thermal model is implemented using C++ libraries within the Solver platform. A typical thermal history output from the simulation is shown in Figure 14 below, which contains several peaks. The first temperature peak occurs when the topmost part is melted using the layer heat source. The temperature then drops during

the recoating time. The next peak occurs when the next layer is deposited, and a high temperature value is observed just above the probed material point. Further temperature peaks are experienced when the material point just above, in the freshly deposited layer, goes through the same cycle.

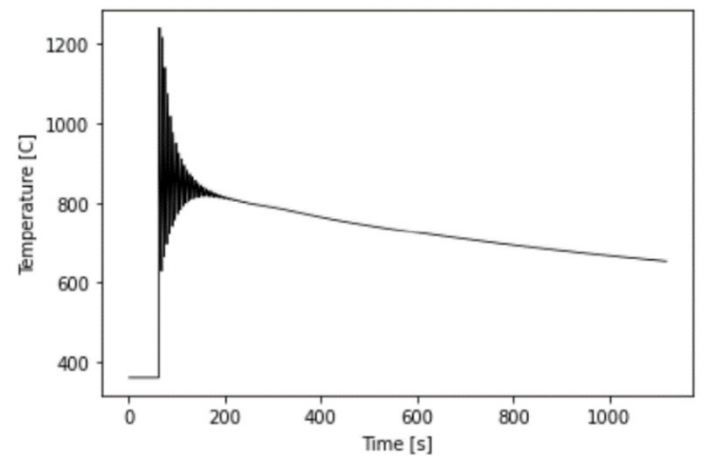


Figure 14: Predicted thermal history output

To detect overheating, the first peak of the thermal history for each material point is used as an indicator. The first peak for each material point is recorded and overlaid on the AM part to provide a 'hotspot map' for the geometry. An example of such a hotspot map is shown I Figure 15 below, where the region above the circular feature is identified as hotspots, in line with practical experience where overhanging features are known to cause overheating.

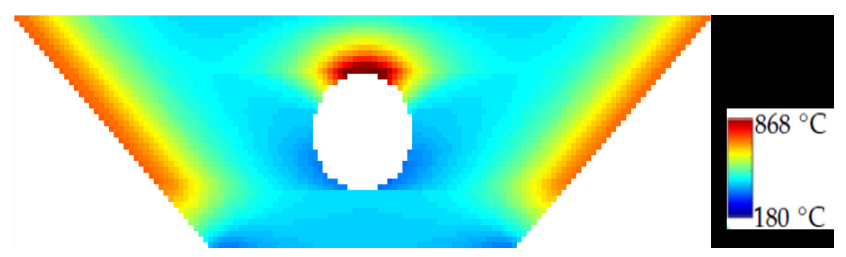


Figure 15: A predicted hotspot map showing the occurrence of heat accumulation

Alloyed's Solver offers a multiple fidelity approach by keeping the Boundary Value Problem the same, while introducing simplifications for each mode to gain in the computational costs:

5.1 Transient mode:

This is a transient analysis with layer-by-layer material addition. A

heat sink boundary condition is assumed at the bottom of the part, symbolising the baseplate, while convection and radiation are specified for the top layer. The power around the part is not considered due to its low conductivity. This mode is the most computationally intensive but provides the highest level of accuracy.

5.2 Static mode:

For a quick design check, this mode is introduced where the BCs for the transient mode remain valid while a steady state analysis is performed on a local domain to solve the PDE. This gives fast results, but temperatures do not retain their physical values. A high hotspot index value indicates a high probability of overheating. Figure 5, shown previously, shows the result of the simplified model applied to the bubble ring. The result of the simplified thermal model shows that the hotspot indices are consistent with the detection of thermal accumulation and therefore remain suitable for rapid pre-AM manufacturing analysis.

References

Atkin, R. (1996). Troubleshooting Platinum Casting Defects and Difficulties. *Proc Santa Fe Symposium*, D, 327–337.

Ferraro, M. (2023). Additive Manufacturing in the jewellery industry: exploring the potential of platinum and titanium. *Metal AM*, 9(4), 139–144. https://www.metal-am.com/metal-additive-manufacturing-magazine-archive/metal-additive-manufacturing-vol-9-no-4-winter-2023/

Fletcher, D. (2018). The Precious Project: Polishing and Finishing of Additive Manufacturing (AM) Jewelry. *Proc Sante Fe Symposium*, 211–234.

Frye, T., & Fischer-Buehner, J. (2012). The quest for quality: Optimising platinum casting for 21st century needs. *Platinum Metals Review*, 56(3), 155–161. https://doi.org/10.1595/147106712X648940

Frye, T., Lisin, M., Meltzer, J., & Mueller, K. (2023). Mechanical Properties and Microstructures of Additively Manufactured 950 Platinum Ruthenium Alloy. *The Jewelry Symposium* 2023 (Minneapolis).

Held, F., & Klotz, U. E. (2022). Effect of Material Properties and Process Parameters in Powder Bed Additive Manufacturing. *Proc. Sante Fe Symposium*, 233–262.

ISO/ASTM 52900. (2021). Additive manufacturing — General principles — Terminology.

Jörg Fischer-Bühner, D.-I. (2023). Platinum Powder for Additive Manufacturing of Jewelry. *The Jewelry Symposium* 2023 (Minneapolis).

Klotz, U. E., & König, F. R. (2022). Additive Manufacturing of Platinum Alloys: Practical aspects during laser powder bed fusion of jewellery items. *Johnson Matthey Technology Review*, 67(3), 303–316. https://doi.org/10.1595/205651323x16691084445762

Laag, T., & Heinrich, J. (2018). Advantages and Challenges of Platinum Group Metals Powder Processing. *Sante Fe Symposium*, 327–343. https://www.dropbox.com/s/l48mivww79m4poo/Laag_Thomas.pdf?e=1&dl=0

Ranjan, R., Ayas, C., Langelaar, M., & van Keulen, F. (2020). Fast detection of heat accumulation in powder bed fusion using computationally efficient thermal models. *Materials*, 13(20), 1–25. https://doi.org/10.3390/ma13204576

Zito, D., Allodi, V., Trevisan, F., Maria Grazia Malagoli Rossini, Rossini, A., & Mazza, M. (2018). Potential and Innovation of Selective Laser Melting Technique in Platinum Jewelry Production. Proc. *Sante Fe Symposium*, 625–684.

Zito, D., Carlotto, A., Loggi, A., Sbornicchia, P., Bruttomesso, D., & Rappo, S. (2015). Definition and solidity of gold and platinum jewels produced using Selective Laser Melting SLMTM technology. *Proc Sante Fe Symposium*. https://www.progold.com/PG_Resources/PG_Documents/Innovation/SFS2015_GB.pdf

Zito, D., Saccardo, E., Sbornicchia, P., Allodi, V., Cepeda, G. A., & Progold, A. (2022). *Innovative Printing Strategy for High-Resolution Jewelry Production by Selective Laser Melting*.